Computational Mechanics 31 (2003) 367–377 © Springer-Verlag 2003
DOI 10.1007/s00466-003-0439-y

Conjugate gradient-boundary element solution to the Cauchy problem for Helmholtz-type equations

L. Marin, L. Elliott, P. J. Heggs, D. B. Ingham, D. Lesnic, X. Wen

Abstract In this paper, an iterative algorithm based on the conjugate gradient method (CGM) in combination with the boundary element method (BEM) for obtaining stable approximate solutions to the Cauchy problem for Helmholtz-type equations is analysed. An efficient regularising stopping criterion for CGM proposed by Nemirovskii [25] is employed. The numerical results obtained confirm that the CGM + BEM produces a convergent and stable numerical solution with respect to increasing the number of boundary elements and decreasing the amount of noise added into the input data.

Keywords Inverse problem, Cauchy problem, Helmholtz-type equations, CGM, BEM

1 Introduction

The Helmholtz equation arises naturally in many physical applications related to wave propagation and vibration phenomena. It is often used to describe the vibration of a structure [1], the acoustic cavity problem [2], the radiation wave [3] and the scattering of a wave [4]. Another important application of the Helmholtz equation is the problem of heat conduction in fins, see e.g. Kern and Kraus [5] and Manzoor et al. [6].

The knowledge of the Dirichlet, Neumann or mixed boundary conditions on the entire boundary of the solution domain gives rise to direct problems for the Helmholtz equation which have been extensively studied in the literature. For example, Niwa et al. [8] have studied the solution to the Helmholtz equation using the complex valued boundary element method (BEM). De Mey [9] has proposed a simplified formulation which used the real part of the complex valued fundamental solution to construct the real part BEM for the Helmholtz equation. Hutchinson [10] has used the real part BEM in order to solve the vibration problems of a membrane. Later, other real-valued formulations have been developed, e.g. the multiple reciprocity method (MRBEM) [11, 12, 13] and the dual reciprocity method (DRBEM) [14, 15, 16].

The well-posedness of the direct problems of the Helmholtz equation via the removal of the eigenvalues of the Laplacian operator is well established, see e.g. Chen and Zhou [17]. Unfortunately, many engineering problems do not belong to this category. In particular, the boundary conditions are often incomplete, either in the form of underspecified and overspecified boundary conditions on different parts of the boundary or the solution is prescribed at some internal points in the domain. These are inverse problems, and it is well known that they are generally ill-posed, i.e. the existence, uniqueness and stability of their solutions are not always guaranteed.

There are important studies of the Cauchy problem for the Helmholtz equation in the literature. Unlike in direct problems, the uniqueness of the Cauchy problem is guaranteed without the necessity of removing the eigenvalues for the Laplacian. However, the Cauchy problem suffers from the non-existence of the solution and continuous dependence on the input data. A BEM-based acoustic holography technique using the singular value decomposition (SVD) for the reconstruction of sound fields generated by irregularly shaped sources has been developed by Bai [18]. The vibrational velocity, sound pressure and acoustic power on the vibrating boundary comprising an enclosed space have been reconstructed by Kim and Ih [19] who have used the SVD in order to obtain the inverse solution in the least-squares sense and to express the acoustic modal expansion between the measurement and source field. Wang and Wu [20] have developed a method employing the spherical wave expansion theory and a least-squares minimisation to reconstruct the acoustic pressure field from a vibrating object and their method has been extended to the reconstruction of acoustic pressure fields inside the cavity of a vibrating object by Wu and Yu [21]. Recently, DeLillo et al. [22] have detected the source of acoustical noise inside the cabin of a midsize aircraft from measurements of the acoustical pressure field inside the cabin by solving a linear Fredholm integral equation of the first kind.

Received: 5 November 2002 / Accepted: 5 March 2003

L. Marin (✉), X. Wen
School of the Environment, University of Leeds,
Leeds LS2 9JT, UK
E-mail: liviu@env.leeds.ac.uk

L. Elliott, D. B. Ingham, D. Lesnic
Department of Applied Mathematics,
University of Leeds, Leeds LS2 9JT, UK

P. J. Heggs
Department of Chemical Engineering,
UMIST, P.O. Box 88,
Manchester M60 1QD, UK

L. Marin would like to acknowledge the financial support received from the EPSRC. The authors would like to thank Professor Dinh Nho Hào and Dr. Thomas Johansson for some useful discussions and suggestions.

In this paper, we apply a variational method for solving the Cauchy problem for Helmholtz-type equations in a two-dimensional geometry by considering the solution on the underspecified boundary as a control in a direct mixed well-posed problem while trying to fit the Cauchy data on the overspecified boundary. In doing so, we attempt to minimise a functional relating the discrepancies between the known and calculated values of the data on the overspecified boundary following a technique similar to that used by Hào and Lesnic [23] and Marin et al. [24] for the Cauchy problem for the Laplace equation and the Lamé system, respectively. We prove that this functional is twice Fréchet differentiable and a formula for the gradient of the functional is obtained via some appropiate adjoint problems. Since the minimisation problem contains almost all the properties of the Cauchy problem it still remains ill-posed. The conjugate gradient method (CGM), with a stopping rule proposed by Nemirovskii [25], is therefore employed. This method is known to have an optimal order convergence rate, see Nemirovskii [25]. The numerical implementation of the CGM is based on the BEM.

2
Mathematical formulation

Consider an open bounded domain $\Omega \subset \mathbb{R}^d$, where d is the dimension of the space in which the problem is posed, usually $d \in \{1,2,3\}$, and assume that Ω is bounded by a surface $\Gamma = \partial\Omega \in \mathscr{C}^1$. We also assume that the boundary consists of two parts, $\Gamma = \Gamma_1 \cup \Gamma_2$, where $\Gamma_1, \Gamma_2 \neq \emptyset$ and $\Gamma_1 \cap \Gamma_2 = \emptyset$.

Referring to heat transfer for the sake of the physical explanation, we assume that the temperature field $T(\underline{x})$ satisfies the Helmholtz-type equation in the domain Ω, namely

$$LT(\underline{x}) \equiv (\Delta + \mathscr{K}^2)T(\underline{x}) = 0, \quad \underline{x} \in \Omega \ , \tag{1}$$

where $\mathscr{K} = \alpha + i\beta \in \mathbb{C}$, $i = \sqrt{-1}$, $\alpha = 0$ and $\beta \in \mathbb{R}$. For example, Eq. (1) models the heat conduction in a fin, see e.g. Kern and Kraus [5], Manzoor et al. [6] and Lin and Jang [7], where T is the dimensionless local fin temperature, $\beta^2 = h/(\tilde{k}t)$, h is the surface heat transfer coefficient [W/(m^2 K)], $\tilde{k}$ is the thermal conductivity of the fin [W/(m K)] and t is the half-fin thickness [m]. The variational method described in the next section is also valid in the case when $\mathscr{K}$ is real, i.e. $\alpha \in \mathbb{R}$ and $\beta = 0$.

Let $n(\underline{x})$ be the outward unit normal vector at Γ and $\frac{\partial T}{\partial n}(\underline{x}) \equiv (\nabla T \cdot n)(\underline{x})$ be the flux at a point $\underline{x} \in \Gamma$. In the direct problem formulation, the knowledge of the temperature and/or flux on the whole boundary Γ gives the corresponding Dirichlet, Neumann, or mixed boundary conditions which enables us to determine the temperature distribution in the domain Ω. If it is possible to measure both the temperature and the flux on a part of the boundary Γ, say Γ_2, then this leads to the mathematical formulation of an inverse problem consisting of equation (1) and the boundary conditions

$$T(\underline{x}) = \tilde{T}(\underline{x}), \quad \frac{\partial T}{\partial n}(\underline{x}) = \tilde{\Phi}(\underline{x}), \quad \underline{x} \in \Gamma_2 \ , \tag{2}$$

where $\tilde{T}$ and $\tilde{\Phi}$ are prescribed functions. In the above formulation of the boundary conditions (2), it can be seen that the boundary Γ_2 is overspecified by prescribing both the temperature $T|_{\Gamma_2}$ and the flux $\partial T/\partial n|_{\Gamma_2}$, whilst the boundary Γ_1 is underspecified since both the temperature $T|_{\Gamma_1}$ and the flux $\partial T/\partial n|_{\Gamma_1}$ are unknown and have to be determined. It should be noted that the problem studied in this paper is of practical importance. For example, the Cauchy problem (1) and (2), where $\mathscr{K} \in \mathbb{C}\backslash\mathbb{R}$, represents the mathematical model for the heat conduction in plate finned-tube heat exchangers, see [5, 6, 7], for which the temperature and the flux can be measured at some points on the fin, whilst both the temperature and the flux are unknown at the fin base or, equivalently, in the tubes.

This problem, termed the Cauchy problem, is much more difficult to solve both analytically and numerically than the direct problem, since the solution does not satisfy the general conditions of well-posedness. In addition, it should be stressed that the Dirichlet, Neumann or mixed direct problems associated to equation (1) do not always have a unique solution due to the eigensolutions, see Chen and Zhou [17]. However, the Cauchy problem given by equations (1) and (2) has a unique solution based on the analytical continuation property. Although this problem has a unique solution, it is well known that this solution is unstable with respect to small perturbations in the data on Γ_2, see e.g. Hadamard [26]. Thus the problem under investigation is ill-posed and we cannot use a direct approach, such as the Gauss elimination method, in order to solve the system of linear equations which arises from the discretisation of the partial differential equations (1) and the boundary conditions (2). Therefore, knowing the exact data $\tilde{T}$ and $\tilde{\Phi}$ on the boundary Γ_2, we apply a variational method to the aforementioned Cauchy problem.

3
Variational method

The Cauchy problem under investigation is given by Eqs. (1) and (2), where $\tilde{T} \in L^2(\Gamma_2)$, $\tilde{\Phi} \in L^2(\Gamma_2)$ and T is sought in $H^{1/2}(\Omega)$. We note that $\tilde{\Phi} \in H^{-1}(\Gamma_1)$ is sufficient for this variational method. Let us denote by $\gamma_j f$ the trace of a function f determined in Ω over Γ_j, $j = 1,2$. First we solve the direct problem

$$\begin{cases} LT(\underline{x}) = 0, & \underline{x} \in \Omega \\ \gamma_1 T(\underline{x}) = v(\underline{x}), & \underline{x} \in \Gamma_1 \\ \gamma_2 \frac{\partial T}{\partial n}(\underline{x}) = \tilde{\Phi}(\underline{x}), & \underline{x} \in \Gamma_2 \end{cases} \tag{3}$$

with $v \in H^{1/2}(\Gamma_1)$. If we denote by $T = T(v, \tilde{\Phi})$ the solution to the problem (3) and define the linear operator

$$A : H^{1/2}(\Gamma_1) \longrightarrow L^2(\Gamma_2), \quad v \longrightarrow Av \equiv \gamma_2 T(v, \tilde{\Phi}) \ , \tag{4}$$

then we aim to find $v \in H^{1/2}(\Gamma_1)$ such that

$$Av \equiv \gamma_2 T(v, \tilde{\Phi}) = \tilde{T} \ . \tag{5}$$

To do so, we attempt to minimise the functional

$$\begin{aligned} J : H^{1/2}(\Gamma_1) &\longrightarrow [0, \infty), \\ v \longrightarrow J(v) &\equiv \tfrac{1}{2}\|Av - \tilde{T}\|_{L^2(\Gamma_2)} \\ &= \tfrac{1}{2}\|\gamma_2 T(v, \tilde{\Phi}) - \tilde{T}\|_{L^2(\Gamma_2)} \end{aligned} \tag{6}$$

with respect to $v \in H^{1/2}(\Gamma_1)$, i.e.

Find $v^* \in H^{1/2}(\Gamma_1)$ such that $J(v^*) = \min_{v \in H^{1/2}(\Gamma_1)} J(v)$.

(7)

We note that since $v \in H^{1/2}(\Gamma_1)$, $\tilde{\Phi} \in L^2(\Gamma_2)$ and $\Gamma \in \mathscr{C}^1$ there is a unique solution $T(v, \tilde{\Phi}) \in H^{1/2}(\Omega)$ of the direct problem (3), see e.g. Lions and Magenes [27]. Thus $Av \equiv \gamma_2 T(v, \tilde{\Phi}) \in L^2(\Gamma_2)$ and hence expression (5) is meaningful.

In what follows we need the following result on Green's formula:

Consider now the problem

$$\begin{cases} L\Psi(\underline{x}) = 0, & \underline{x} \in \Omega \\ \gamma_1 \Psi(\underline{x}) = 0, & \underline{x} \in \Gamma_1 \\ \gamma_2 \frac{\partial \Psi}{\partial n}(\underline{x}) = q(\underline{x}), & \underline{x} \in \Gamma_2 \end{cases} \tag{8}$$

with $q \in L^2(\Gamma_2)$.

Lemma 1 Let T and Ψ be the solutions of the problems (3) and (8), respectively. Then

$$\int_{\Gamma_1} \gamma_1 \frac{\partial \Psi}{\partial n}(\underline{x}) v(\underline{x}) \mathrm{d}\Gamma(\underline{x}) + \int_{\Gamma_2} q(\underline{x}) \gamma_2 T(\underline{x}) \mathrm{d}\Gamma(\underline{x}) = \int_{\Gamma_2} \tilde{\Phi}(\underline{x}) \gamma_2 \Psi(\underline{x}) \mathrm{d}\Gamma(\underline{x}) \ . \tag{9}$$

Proof: We note that since $q \in L^2(\Gamma_2)$, then $\Psi \in H^{3/2}(\Omega)$ and hence, $\gamma_1 \partial\Psi/\partial n \in L^2(\Gamma_1)$. It follows that relation (9) is meaningful in the classical sense. This can be proved in the framework of distribution theory, see e.g. Lions and Magenes [27], but an alternative proof is given here.

Let $v^{(n)} \in H^1(\Gamma_1)$ be a sequence such that $v^{(n)} \longrightarrow v$ in $H^{1/2}(\Gamma_1)$. We denote by $T^{(n)} = T(v^{(n)}, \tilde{\Phi})$ the solution of the problem (3) with $v = v^{(n)}$. It can be proved, see e.g. Lions and Magenes [27], that $T^{(n)} \in H^{3/2}(\Omega)$ and $T^{(n)} \longrightarrow T$ in $H^{1/2}(\Omega)$. It follows that $\gamma_2 T^{(n)} \longrightarrow \gamma_2 T$ in $L^2(\Gamma_2)$. Since $\Psi \in H^{3/2}(\Omega)$, we have

$$\begin{aligned} 0 &= \int_\Omega L T^{(n)}(\underline{x}) \Psi(\underline{x}) \mathrm{d}\Omega(\underline{x}) \\ &= \int_\Gamma \frac{\partial T^{(n)}}{\partial n}(\underline{x}) \Psi(\underline{x}) \mathrm{d}\Gamma(\underline{x}) \\ &\quad - \int_\Omega \left(\frac{\partial T^{(n)}}{\partial x_j}(\underline{x}) \frac{\partial \Psi}{\partial x_j}(\underline{x}) - \mathscr{K}^2 T^{(n)}(\underline{x}) \Psi(\underline{x}) \right) \mathrm{d}\Omega(\underline{x}) \\ &= \int_{\Gamma_1} \gamma_1 \frac{\partial T^{(n)}}{\partial n}(\underline{x}) \gamma_1 \Psi(\underline{x}) \mathrm{d}\Gamma(\underline{x}) \\ &\quad + \int_{\Gamma_2} \gamma_2 \frac{\partial T^{(n)}}{\partial n}(\underline{x}) \gamma_2 \Psi(\underline{x}) \mathrm{d}\Gamma(\underline{x}) \\ &\quad - \int_\Omega \left(\frac{\partial T^{(n)}}{\partial x_j}(\underline{x}) \frac{\partial \Psi}{\partial x_j}(\underline{x}) - \mathscr{K}^2 T^{(n)}(\underline{x}) \Psi(\underline{x}) \right) \mathrm{d}\Omega(\underline{x}) \ . \end{aligned} \tag{10}$$

If we now substitute the boundary conditions from both problems (3) and (8) into the surface integrals in (10), we obtain

$$\begin{aligned} &\int_\Omega \left(\frac{\partial T^{(n)}}{\partial x_j}(\underline{x}) \frac{\partial \Psi}{\partial x_j}(\underline{x}) - \mathscr{K}^2 T^{(n)}(\underline{x}) \Psi(\underline{x}) \right) d\Omega(\underline{x}) \\ &\quad = \int_{\Gamma_2} \tilde{\Phi}(\underline{x}) \gamma_2 \Psi(\underline{x}) \mathrm{d}\Gamma(\underline{x}) \ . \end{aligned} \tag{11}$$

In a similar manner, since $T^{(n)} \in H^{3/2}(\Omega)$, we have

$$\begin{aligned} 0 &= \int_\Omega L\Psi(\underline{x}) T^{(n)}(\underline{x}) \mathrm{d}\Omega(\underline{x}) \\ &= \int_\Gamma \frac{\partial \Psi}{\partial n}(\underline{x}) T^{(n)}(\underline{x}) \mathrm{d}\Gamma(\underline{x}) \\ &\quad - \int_\Omega \left(\frac{\partial T^{(n)}}{\partial x_j}(\underline{x}) \frac{\partial \Psi}{\partial x_j}(\underline{x}) - \mathscr{K}^2 T^{(n)}(\underline{x}) \Psi(\underline{x}) \right) \mathrm{d}\Omega(\underline{x}) \\ &= \int_{\Gamma_1} \gamma_1 \frac{\partial \Psi}{\partial n}(\underline{x}) \gamma_1 T^{(n)}(\underline{x}) \mathrm{d}\Gamma(\underline{x}) \\ &\quad + \int_{\Gamma_2} \gamma_2 \frac{\partial \Psi}{\partial n}(\underline{x}) \gamma_2 T^{(n)}(\underline{x}) \mathrm{d}\Gamma(\underline{x}) \\ &\quad - \int_\Omega \left(\frac{\partial T^{(n)}}{\partial x_j}(\underline{x}) \frac{\partial \Psi}{\partial x_j}(\underline{x}) - \mathscr{K}^2 T^{(n)}(\underline{x}) \Psi(\underline{x}) \right) \mathrm{d}\Omega(\underline{x}) \ . \end{aligned} \tag{12}$$

If we now substitute the boundary conditions from both problems (3) and (8) into the surface integrals in (12), we obtain

$$\begin{aligned} &\int_\Omega \left(\frac{\partial T^{(n)}}{\partial x_j}(\underline{x}) \frac{\partial \Psi}{\partial x_j}(\underline{x}) - \mathscr{K}^2 T^{(n)}(\underline{x}) \Psi(\underline{x}) \right) \mathrm{d}\Omega(\underline{x}) \\ &= \int_{\Gamma_1} \gamma_1 \frac{\partial \Psi}{\partial n}(\underline{x}) v^{(n)}(\underline{x}) \mathrm{d}\Gamma(\underline{x}) \\ &\quad + \int_{\Gamma_2} q(\underline{x}) \gamma_2 T^{(n)}(\underline{x}) \mathrm{d}\Gamma(\underline{x}) \ . \end{aligned} \tag{13}$$

From relations (11) and (13), we obtain

$$\int_{\Gamma_1} \gamma_1 \frac{\partial \Psi}{\partial n}(\underline{x}) v^{(n)}(\underline{x}) \mathrm{d}\Gamma(\underline{x}) + \int_{\Gamma_2} q(\underline{x}) \gamma_2 T^{(n)}(\underline{x}) \mathrm{d}\Gamma(\underline{x}) = \int_{\Gamma_2} \tilde{\Phi}(\underline{x}) \gamma_2 \Psi(\underline{x}) \mathrm{d}\Gamma(\underline{x}) \ . \tag{14}$$

Letting $n \longrightarrow \infty$ in (14) we establish relation (9) and hence Lemma 1 is proved. □

Now we are in a position to consider the variational problem. The first result concerning the approximate controllability is as follows:

Theorem 1 *The set* $\{\gamma_2 T(v, \tilde{\Phi}) | v \in H^{1/2}(\Gamma_1)\}$ *is dense in* $L^2(\Gamma_2)$, *i.e. the Cauchy problem (1) and (2) is solvable in* $H^{1/2}(\Omega)$ *for almost all* $T, \tilde{\Phi} \in L^2(\Gamma_2)$.

Proof: Let $\eta \in L^2(\Gamma_2)$ be such that

$$\int_{\Gamma_2} \gamma_2 T(v, \tilde{\Phi})(\underline{x}) \eta(\underline{x}) \mathrm{d}\Gamma(\underline{x}) = 0, \quad \forall v \in H^{1/2}(\Gamma_1) \ . \tag{15}$$

Let $\Psi(0, \eta)$ be the solution of the problem (8) with $q = \eta$. Then we have $\gamma_2 \Psi \in L^2(\Gamma_2)$. From Green's formula (9) and expression (15) we obtain

$$\int_{\Gamma_1} \gamma_1 \frac{\partial \Psi(0,\eta)}{\partial n}(\underline{x}) v(\underline{x}) \mathrm{d}\Gamma((\underline{x}) = \int_{\Gamma_2} \tilde{\Phi}(\underline{x}) \gamma_2 \Psi(0,\eta)(\underline{x}) \mathrm{d}\Gamma(\underline{x}), \quad \forall v \in H^{1/2}(\Gamma_1) \ . \tag{16}$$

Replacing v with $-v$ in (16), we obtain

$$-\int_{\Gamma_1} \gamma_1 \frac{\partial \Psi(0,\eta)}{\partial n}(\underline{x}) v(\underline{x}) \mathrm{d}\Gamma((\underline{x}) = \int_{\Gamma_2} \tilde{\Phi}(\underline{x}) \gamma_2 \Psi(0,\eta)(\underline{x}) \mathrm{d}\Gamma(\underline{x}), \quad \forall v \in H^{1/2}(\Gamma_1) \ . \tag{17}$$

Equations (16) and (17) imply that

$$\int_{\Gamma_1} \gamma_1 \frac{\partial \Psi(0,\eta)}{\partial n}(\underline{x}) v(\underline{x}) \mathrm{d}\Gamma((\underline{x}) = 0, \quad \forall v \in H^{1/2}(\Gamma_1)$$

and hence we have

$$\gamma_1 \frac{\partial \Psi(0,\eta)}{\partial n}(\underline{x}) = 0, \quad \underline{x} \in \Gamma_1 \ .$$

Thus, the function $\Psi(0,\eta) \in H^{3/2}(\Omega)$ satisfies the problem given by (1) and the boundary conditions $\gamma_1 \Psi(0,\eta)(\underline{x}) = \gamma_1 \partial \Psi(0,\eta)/\partial n(\underline{x}) = 0$, $\underline{x} \in \Gamma_1$. From a uniqueness theorem for the Cauchy problem of the Helmholtz equation, it follows that $\Psi(0,\eta) \equiv 0$ and therefore $\gamma_2 \Psi(0,\eta)(\underline{x}) = \eta(\underline{x}) = 0$, $\underline{x} \in \Gamma_2$. Thus the theorem is proved. □

Furthermore, we have the following result:

Corollary 1

$$\inf_{v \in H^{1/2}(\Gamma_1)} J(v) = 0 \ .$$

Theorem 2 *The functional $J(v)$ is twice Fréchet differentiable and is strictly convex. Moreover, its first gradient has the form*

$$J'(v) = -\gamma_1 \frac{\partial \Psi}{\partial n} \ . \tag{18}$$

Proof: Let η be a function in $H^{1/2}(\Gamma_1)$ and denote by $\langle \cdot, \cdot \rangle_{L^2(\Gamma_2)}$ the scalar product in the space $L^2(\Gamma_2)$. Then using relations (5) and (6) we have

$$\begin{aligned} J(v+\eta) - J(v) &= \frac{1}{2} \|A(v+\eta) - \tilde{T}\|^2_{L^2(\Gamma_2)} \\ &\quad - \frac{1}{2} \|Av - \tilde{T}\|^2_{L^2(\Gamma_2)} \\ &= \frac{1}{2} \|\gamma_2 T(v+\eta, \tilde{\Phi}) - \tilde{T}\|^2_{L^2(\Gamma_2)} \\ &\quad - \frac{1}{2} \|\gamma_2 T(v, \tilde{\Phi}) - \tilde{T}\|^2_{L^2(\Gamma_2)} \ . \end{aligned} \tag{19}$$

The linearity of the boundary value problems for the Helmholtz equation implies the validity of the superposition principle, so that we have $T(v+\eta, \tilde{\Phi}) = T(v, \tilde{\Phi}) + T(\eta, 0)$, where we have denoted by $T(\eta, 0)$ the solution to the following direct problem

$$\begin{cases} LT(\eta,0)(\underline{x}) = 0, & \underline{x} \in \Omega \\ \gamma_1 T(\eta,0)(\underline{x}) = \eta(\underline{x}), & \underline{x} \in \Gamma_1 \\ \gamma_2 \frac{\partial T(\eta,0)}{\partial n}(\underline{x}) = 0, & \underline{x} \in \Gamma_2 \ . \end{cases} \tag{20}$$

Thus (19) can be written in the following form:

$$J(v+\eta) - J(v) = \left\langle \gamma_2 T(v, \tilde{\Phi}) - \tilde{T}, \gamma_2 T(\eta, 0) \right\rangle_{L^2(\Gamma_2)} + \frac{1}{2} \|\gamma_2 T(\eta, 0)\|^2_{L^2(\Gamma_2)} \ . \tag{21}$$

Let us consider now the adjoint problem, namely

$$\begin{cases} L\Psi(\underline{x}) = 0, & \underline{x} \in \Omega \\ \gamma_1 \Psi(\underline{x}) = 0, & \underline{x} \in \Gamma_1 \\ \gamma_2 \frac{\partial \Psi}{\partial n}(\underline{x}) = \gamma_2 T(v, \tilde{\Phi})(\underline{x}) - \tilde{T}(\underline{x}), & \underline{x} \in \Gamma_2 \ . \end{cases} \tag{22}$$

Applying Green's formula (9) to the problems (20) and (22), we obtain

$$-\int_{\Gamma_1} \gamma_1 \frac{\partial \Psi}{\partial n}(\underline{x}) \eta(\underline{x}) \mathrm{d}\Gamma(\underline{x}) = \int_{\Gamma_2} \left(\gamma_2 T(\eta,0)(\underline{x}) - \tilde{T}(\underline{x}) \right) \gamma_2 T(\eta,0)(\underline{x}) \mathrm{d}\Gamma(\underline{x})$$

and, consequently, from (21) we have

$$J(v+\eta) - J(v) = -\int_{\Gamma_1} \gamma_1 \frac{\partial \Psi}{\partial n}(\underline{x}) \eta(\underline{x}) \mathrm{d}\Gamma(\underline{x}) + \frac{1}{2} \|\gamma_2 T(\eta, 0)\|^2_{L^2(\Gamma_2)} \ . \tag{23}$$

Since $T(\eta, 0)$ is the solution in $H^{1/2}(\Omega)$ to the problem (20), then there exists a constant $c > 0$ such that

$$\|T(\eta,0)\|_{H^{1/2}(\Omega)} \leq c \|\eta\|_{H^{1/2}(\Gamma_1)} \ .$$

It follows immediately that

$$\|\gamma_2 T(\eta,0)\|^2_{L^2(\Gamma_2)} \longrightarrow 0 \quad \text{as} \quad \|\eta\|_{H^{1/2}(\Gamma_1)} \longrightarrow 0$$

which means that the functional $J(v)$ is Fréchet differentiable and its first gradient is given by (18).

Consider now the problem

$$\begin{cases} L\varphi(\underline{x}) = 0, & \underline{x} \in \Omega \\ \gamma_1 \varphi(\underline{x}) = 0, & \underline{x} \in \Gamma_1 \\ \gamma_2 \frac{\partial \varphi}{\partial n}(\underline{x}) = \gamma_2 T(\eta,0)(\underline{x}), & \underline{x} \in \Gamma_2 \ , \end{cases} \tag{24}$$

which has a unique solution in $H^{3/2}(\Omega)$ since $\gamma_2 T(\eta, 0) \in L^2(\Gamma_2)$. If we apply Green's formula (9) to the problems (20) and (24), we obtain

$$\int_{\Gamma_2} \gamma_2 T(\eta,0)(\underline{x}) \gamma_2 T(\eta,0)(\underline{x}) \mathrm{d}\Gamma(\underline{x}) = -\int_{\Gamma_1} \gamma_1 \frac{\partial \varphi}{\partial n}(\underline{x}) \eta(\underline{x}) \mathrm{d}\Gamma(\underline{x}) \tag{25}$$

and it follows that the functional $J(v)$ is twice Fréchet differentiable and its second gradient is given by the formula

$$J''(v) \cdot \eta = -\gamma_1 \frac{\partial \varphi}{\partial n} \ .$$

In order to prove that the functional $J(v)$ is strictly convex, we first observe that $J(v)$ is convex since

$$\langle J''(v)\cdot\eta,\eta\rangle_{L^2(\Gamma_2)} = -\int_{\Gamma_1}\gamma_1\frac{\partial\varphi}{\partial n}(\underline{x})\eta(\underline{x})\mathrm{d}\Gamma(\underline{x})$$

and, according to (25), we have

$$\begin{aligned}\langle J''(v)\cdot\eta,\eta\rangle_{L^2(\Gamma_2)} &= \int_{\Gamma_2}|\gamma_2 T(\eta,0)(\underline{x})|^2\mathrm{d}\Gamma(\underline{x})\\ &= \|\gamma_2 T(\eta,0)\|^2_{L^2(\Gamma_2)}\geq 0\ .\end{aligned}$$

Further, if $\langle J''(v)\cdot\eta,\eta\rangle_{L^2(\Gamma_2)}=0$, then $\gamma_2 T(\eta,0)(\underline{x})=0$ and it follows that $T(\eta,0)$ satisfies the problem

$$\begin{cases} LT(\eta,0)(\underline{x})=0, & \underline{x}\in\Omega\\ \gamma_2 T(\eta,0)(\underline{x})=0, & \underline{x}\in\Gamma_2\\ \gamma_2\frac{\partial T(\eta,0)}{\partial n}(\underline{x})=0, & \underline{x}\in\Gamma_2\ . \end{cases}$$

From a theorem on the uniqueness of the Cauchy problem of the Helmholtz equation, we have that $T(\eta,0)\equiv 0$ in Ω. Hence $\eta\equiv 0$ and the functional $J(v)$ is strictly convex. □

Theorem 3 *(i) If there exists a solution $v^*\in H^{1/2}(\Gamma_1)$ of the variational problem (7), then it is unique. Furthermore, $J(v^*)=0$ and from this it follows that the Cauchy problem given by equations* (1)*and*(2) *has a unique solution in $H^{1/2}(\Omega)$.* (ii) *If the Cauchy problem given by equations* (1)*and*(2) *has a unique solution in $H^{1/2}(\Omega)$, then there exists a solution $v^*\in H^{1/2}(\Gamma_1)$ of the variational problem* (7).

Proof: (*i*) If the variational problem (7) has a solution $v^*\in H^{1/2}(\Gamma_1)$ then, according to Corollary 1, $J(v^*)=0$. The uniqueness of v^* follows from the strict convexity of the functional J.

(*ii*) This is obvious. □

4
Conjugate gradient method

As we can calculate the gradient of the functional $J(v)$ via the adjoint problem (22), we can now apply the CGM with a stopping rule, as proposed by Nemirovskii [25]. First, we note that due to the linearity of the boundary value problems of Helmholtz-type equations, the superposition principle can be applied and, therefore, $T(v,\tilde{\Phi}) = T(v,0)+T(0,\tilde{\Phi})$.

We define the linear operator

$$A_0 : H^{1/2}(\Gamma_1)\longrightarrow L^2(\Gamma_2),\quad v\longrightarrow A_0 v\equiv\gamma_2 T(v,0)$$

and thus we have the following linear equation, which is equivalent to (5),

$$\begin{aligned}A_0 v\equiv\gamma_2\big(T(v,\tilde{\Phi})-T(0,\tilde{\Phi})\big) &= \gamma_2 T(v,\tilde{\Phi})-\gamma_2 T(0,\tilde{\Phi})\\ &= \tilde{T}-\gamma_2 T(0,\tilde{\Phi})\equiv\overline{T}\ .\end{aligned}$$

Suppose that instead of $\tilde{T}$ we have only an approximation of it, say $\tilde{T}_\varepsilon\in L^2(\Gamma_2)$ such that

$$\|\tilde{T}-\tilde{T}_\varepsilon\|_{L^2(\Gamma_2)}\leq\varepsilon\ . \tag{26}$$

In order to solve the Cauchy problem given by (1) and (2) with noisy data $\tilde{T}_\varepsilon$, we need to compute $A_0^*(A_0 v-\overline{T}_\varepsilon)$, where A_0^* is the adjoint of the operator A_0 and $\overline{T}_\varepsilon$ is given by

$$\overline{T}_\varepsilon\equiv\tilde{T}_\varepsilon-\gamma_2 T(v,0)\ .$$

However, we observe that this is nothing else than the gradient (18) of the functional (6). Thus the CGM applied to our problem has the form of the following algorithm:

Step 1. Set $k=0$ and choose $v^{(0)}\in H^{1/2}(\Gamma_1)$.

Step 2. Solve the direct problem

$$\begin{cases} LT^{(k)}(\underline{x})=0, & \underline{x}\in\Omega\\ T^{(k)}(\underline{x})=v^{(k)}(\underline{x}), & \underline{x}\in\Gamma_1\\ \frac{\partial T^{(k)}}{\partial n}(\underline{x})=\tilde{\Phi}(\underline{x}), & \underline{x}\in\Gamma_2 \end{cases}$$

to determine the residual

$$r^{(k)}|_{\Gamma_2}=T^{(k)}|_{\Gamma_2}-\tilde{T}_\varepsilon=AT^{(k)}-\tilde{T}_\varepsilon.$$

Step 3. Solve the adjoint problem

$$\begin{cases} L\Psi^{(k)}(\underline{x})=0, & \underline{x}\in\Omega\\ \Psi^{(k)}(\underline{x})=0, & \underline{x}\in\Gamma_1\\ \frac{\partial\Psi^{(k)}}{\partial n}(\underline{x})=r^{(k)}(\underline{x}), & \underline{x}\in\Gamma_2 \end{cases}$$

to determine the gradient $g^{(k)}|_{\Gamma_1}=-\frac{\partial\Psi^{(k)}}{\partial n}|_{\Gamma_1}$. Calculate $d^{(k)}$ as follows:

$$d^{(k)}|_{\Gamma_1}=\begin{cases} g^{(k)}|_{\Gamma_1}, & k=0\\ g^{(k)}|_{\Gamma_1}+\left(\|g^{(k)}\|^2_{H^{1/2}(\Gamma_1)}/\|g^{(k-1)}\|^2_{H^{1/2}(\Gamma_1)}\right)d^{(k-1)}|_{\Gamma_1}, & k\geq 1\ . \end{cases}$$

Step 4. Solve the direct problem

$$\begin{cases} L\varphi^{(k)}(\underline{x})=0, & \underline{x}\in\Omega\\ \varphi^{(k)}(\underline{x})=d^{(k)}(\underline{x}), & \underline{x}\in\Gamma_1\\ \frac{\partial\varphi^{(k)}}{\partial n}(\underline{x})=0, & \underline{x}\in\Gamma_2 \end{cases}$$

to determine $A_0 d^{(k)}=\varphi^{(k)}|_{\Gamma_2}$ and compute

$$v^{(k+1)}|_{\Gamma_1}=v^{(k)}|_{\Gamma_1}+\left(\|g^{(k)}\|^2_{H^{1/2}(\Gamma_1)}/\|A_0 d^{(k)}\|^2_{L^2(\Gamma_2)}\right)d^{(k)}|_{\Gamma_1}\ .$$

Step 5. Set $k=k+1$. Repeat steps 2–4 until a stopping criterion is prescribed.

As a stopping criterion we choose the one suggested by Nemirovskii [25], namely choose the first $k\in\mathbb{N}$ such that

$$\|r^{(k)}\|_{L^2(\Gamma_2)}\leq\delta\varepsilon \tag{27}$$

where $\delta>1$ is a constant which can be taken heuristically to be 1.1, as suggested by Hanke and Hansen [28]. It follows from Nemirovskii's result that the above iterative procedure converges with an optimal convergence rate to the exact solution of the problem as the noise level tends to zero.

We note that in step 2 we have the following relations

$$
\begin{aligned}
r^{(k+1)} &= AT^{(k+1)} - \tilde{T}_\varepsilon = \left(A_0 T^{(k+1)} + \gamma_2 T(0,\tilde{\Phi})\right) - \tilde{T}_\varepsilon \\
&= A_0\left[T^{(k)} + \left(\|g^{(k)}\|^2_{H^{1/2}(\Gamma_1)}/\|A_0 d^{(k)}\|^2_{L^2(\Gamma_2)}\right) d^{(k)}\right] \\
&\quad + \gamma_2 T(0,\tilde{\Phi}) - \tilde{T}_\varepsilon \\
&= \left(\|g^{(k)}\|^2_{H^{1/2}(\Gamma_1)}/\|A_0 d^{(k)}\|^2_{L^2(\Gamma_2)}\right)(A_0 d^{(k)}) \\
&\quad + \left(A_0 T^{(k)} + \gamma_2 T(0,\tilde{\Phi})\right) - \tilde{T}_\varepsilon \\
&= \left(\|g^{(k)}\|^2_{H^{1/2}(\Gamma_1)}/\|A_0 d^{(k)}\|^2_{L^2(\Gamma_2)}\right)(A_0 d^{(k)}) \\
&\quad + (AT^{(k)} - \tilde{T}_\varepsilon) \\
&= \left(\|g^{(k)}\|^2_{H^{1/2}(\Gamma_1)}/\|A_0 d^{(k)}\|^2_{L^2(\Gamma_2)}\right)(A_0 d^{(k)}) + r^{(k)} \quad .
\end{aligned}
$$

Thus we obtain

$$
r^{(k+1)} = r^{(k)} + \left(\|g^{(k)}\|^2_{H^{1/2}(\Gamma_1)}/\|A_0 d^{(k)}\|^2_{L^2(\Gamma_2)}\right)(A_0 d^{(k)}), \quad k \geq 0
$$

and we note that we have in fact to solve only the two direct problems in steps 3 and 4 at every iteration, except for that to determine $r^{(0)}$.

5 Boundary element method

The Helmholtz-type equation (1) can also be formulated in integral form, see e.g. Chen and Zhou [17], as

$$
\begin{aligned}
&c(\underline{x})T(\underline{x}) + \int_\Gamma \frac{\partial E(\underline{x},\underline{y})}{\partial n(\underline{y})} T(\underline{y}) \mathrm{d}\Gamma(\underline{y}) \\
&\quad = \int_\Gamma E(\underline{x},\underline{y}) \frac{\partial T}{\partial n}(\underline{y}) \mathrm{d}\Gamma(\underline{y})
\end{aligned} \tag{28}
$$

for $\underline{x} \in \overline{\Omega} = \Omega \cup \Gamma$, where the first integral is taken in the sense of the Cauchy principal value, $c(\underline{x}) = 1$ for $\underline{x} \in \Omega$ and $c(\underline{x}) = 1/2$ for $\underline{x} \in \Gamma$ (smooth), and E is the fundamental solution for the Helmholtz-type equation (1), which in two-dimensions is given by

$$
E(\underline{x},\underline{y}) = \frac{i}{4} H_0^{(1)}\left(\mathscr{K} r(\underline{x},\underline{y})\right) \quad . \tag{29}
$$

Here $r(\underline{x},\underline{y})$ represents the distance between the load point $\underline{x}$ and the field point $\underline{y}$ and $H_0^{(1)}$ is the Hankel function of order zero of the first kind. It should be noted that in practice the boundary integral equation (28) can rarely be solved analytically and thus a numerical approximation is required.

A BEM with constant boundary elements is used in order to solve the intermediate mixed well-posed boundary value problems resulting from the CGM adopted, which is described in Section 4. Consequently, the boundary Γ is approximated by N straight line segments in a counterclockwise sense along with the temperature and the flux which are considered to be constant and take their values at the midpoint, i.e. the collocation point, also known as the node, of each element. More specifically, we have

$$
\begin{aligned}
&\Gamma \approx \bigcup_{n=1}^{N} \Gamma_n, \quad \Gamma_n = [\underline{y}^{n-1}, \underline{y}^n], \quad n = 1,\ldots,N \\
&\underline{y}^N = \underline{y}^0, \quad \underline{x}^n = (\underline{y}^{n-1} + \underline{y}^n)/2, \quad n = 1,\ldots,N
\end{aligned} \tag{30}
$$

and

$$
\begin{aligned}
&T(\underline{y}) = T(\underline{x}^n), \\
&\frac{\partial T}{\partial n}(\underline{y}) = \frac{\partial T}{\partial n}(\underline{x}^n), \quad \underline{y} \in \Gamma_n, \quad n = 1,\ldots,N \quad .
\end{aligned} \tag{31}
$$

By applying the boundary integral equation (28) at each collocation point $\underline{x}^m$, $m = 1,\ldots,N$, and taking into account the fact that the boundary is always smooth at these points, we arrive at the following system of linear algebraic equations

$$
A\underline{T} = B\underline{\Phi} \tag{32}
$$

where A and B are matrices which depend solely on the geometry of the boundary Γ and the vectors $\underline{T}$ and $\underline{\Phi}$ consist of the discretised values of the temperature and the flux on the boundary Γ, namely

$$
T(m) = T(\underline{x}^m), \qquad \Phi(m) = \frac{\partial T}{\partial n}(\underline{x}^m) \tag{33}
$$

for $m = 1,\ldots,N$, and

$$
\begin{aligned}
A(n,m) &= \delta_{nm}/2 + \int_{\Gamma_n} \frac{\partial E(\underline{x}^m,\underline{y})}{\partial n(\underline{y})} \mathrm{d}\Gamma(\underline{y}), \\
B(n,m) &= \int_{\Gamma_n} E(\underline{x}^m,\underline{y}) \mathrm{d}\Gamma(\underline{y})
\end{aligned} \tag{34}
$$

for $\underline{x}^m \in \tilde{\Gamma}$ and $m,\ n = 1,\ldots,N$, where δ_{nm} is the Kronecker tensor. We note that the sense of the Cauchy principal value assigned to the first integral in the boundary integral equation (28) has meaning only when $\underline{x}^m \in \Gamma_n$, as in the other cases the integral is non-singular.

If the boundaries Γ_1 and Γ_2 are discretised into N_1 and N_2 boundary elements, respectively, such that $N_1 + N_2 = N$, then Eq. (32) represents a system of N linear algebraic equations with $2N$ unknowns. The discretisation of the boundary conditions (2) provides the values of $2N_2$ of the unknowns and the problem reduces to solving a system of N equations with $2N_1$ unknowns which can be generically written as

$$
C\underline{X} = \underline{F} \tag{35}
$$

where $\underline{F}$ is computed using the boundary conditions (2), the matrix C depends solely on the geometry of the boundary Γ and the vector $\underline{X}$ contains the unknown values of the temperature and the flux on the boundary Γ_1.

6 Numerical results and discussion

In this section, we illustrate the numerical results obtained using the CGM proposed in Sect. 4 and the BEM described

in Sect. 5. In addition, we investigate the convergence with respect to the mesh size discretisation and the number of iterations when the data is exact and the stability when the data is perturbed by noise.

6.1 Examples

In order to present the performance of the numerical method proposed, we solve the Cauchy problem (1) and (2) in a smooth two-dimensional geometry, namely the annulus $\Omega = \{\underline{x} = (x_1, x_2) | R_i^2 < x_1^2 + x_2^2 < R_o^2\}$, $R_i = 0.5$ and $R_o = 1.0$. We assume that the boundary Γ of the domain Ω is divided into two disjointed parts, namely $\Gamma_1 = \{\underline{x} \in \Gamma | x_1^2 + x_2^2 = R_i^2\}$ and $\Gamma_2 = \{\underline{x} \in \Gamma | x_1^2 + x_2^2 = R_o^2\}$, and the outer boundary Γ_2 is overspecified by the prescription of both the temperature and the flux while the inner boundary Γ_1 is underspecified with both the temperature and the flux unknown.

We consider the following analytical solutions for the temperature in the domain Ω:

Example 1. ($L \equiv \Delta - \beta^2$, $\beta \in \mathbb{R}$)

$$T^{(\mathrm{an})}(\underline{x}) = \exp(a_1 x_1 + a_2 x_2), \quad \underline{x} = (x_1, x_2) \in \Omega \ , \tag{36}$$

where $\mathscr{K} = \alpha + i\beta$, $\alpha = 0$, $\beta = 2.0$, $a_1 = 1.0$ and $a_2 = \sqrt{\beta^2 - a_1^2}$, which corresponds to a flux on the boundary Γ given by

$$\frac{\partial T^{(\mathrm{an})}}{\partial n}(\underline{x}) = (a_1 n_1(\underline{x}) + a_2 n_2(\underline{x})) T^{(\mathrm{an})}(\underline{x}), \quad \underline{x} = (x_1, x_2) \in \Gamma \ , \tag{37}$$

and

Example 2. ($L \equiv \Delta + \alpha^2$, $\alpha \in \mathbb{R}$)

$$T^{(\mathrm{an})}(\underline{x}) = \cos(a_1 x_1 + a_2 x_2), \quad \underline{x} = (x_1, x_2) \in \Omega \ , \tag{38}$$

where $\mathscr{K} = \alpha + i\beta$, $\alpha = 2.0$, $\beta = 0$, $a_1 = 1.0$ and $a_2 = \sqrt{\alpha^2 - a_1^2}$, which corresponds to a flux on the boundary Γ given by

$$\frac{\partial T^{(\mathrm{an})}}{\partial n}(\underline{x}) = -(a_1 n_1(\underline{x}) + a_2 n_2(\underline{x})) \sin(a_1 x_1 + a_2 x_2), \quad \underline{x} = (x_1, x_2) \in \Gamma \ . \tag{39}$$

The Cauchy problems given by Eqs. (1) and (2) for the aforementioned examples have been solved using the CGM + BEM with constant boundary elements to provide the unspecified boundary temperature. The number of boundary elements used for discretising the boundary Γ was taken to be $N \in \{40, 80, 160\}$ with $N_1 = N_2 = N/2$. Although not presented here, it should be mentioned that the boundary flux $\partial T^{(\mathrm{num})}/\partial n|_{\Gamma_1}$ can be computed after obtaining the boundary temperature $T^{(\mathrm{num})}|_{\Gamma_1}$ by solving either a Dirichlet problem, i.e. Eq. (1) with the boundary conditions $T|_{\Gamma_1} = T^{(\mathrm{num})}|_{\Gamma_1}$ and $T|_{\Gamma_2} = \tilde{T}|_{\Gamma_2}$, or a mixed boundary value problem, i.e. Eq. (1) with the boundary conditions $T|_{\Gamma_1} = T^{(\mathrm{num})}|_{\Gamma_1}$ and $\partial T/\partial n|_{\Gamma_2} = \tilde{\Phi}|_{\Gamma_2}$.

6.2 Direct approach

A good a priori insight into the ill-conditioning of the system of linear equations (35) is given by the condition number of the sensitivity matrix C, namely

$$\mathrm{cond} C = \det(C^{tr} C) \ . \tag{40}$$

For the test examples considered, the condition numbers of the sensitivity matrix C were calculated using the NAG subroutine F03AAF which computes the determinant of a matrix using Crout factorisation with partial pivoting. The condition number (40) for $N = 20$ boundary elements corresponding to both examples 1 and 2 is $O(10^{-216})$. When the number of boundary elements exceeds $N = 20$ then the condition numbers are even smaller and the value of the determinant (40) is too small to be stored in the computer. Therefore, a direct approach to the problem produces a highly unstable solution and this is a reason why other methods, such as the method presented here, have to be employed.

An arbitrary function $v^{(0)} \in H^{1/2}(\Gamma_1)$ may be specified as an initial guess for the temperature on Γ_1. For the examples considered, this initial guess has been chosen as

$$v^{(0)}(\underline{x}) = 0, \quad \underline{x} \in \Gamma_1 \ , \tag{41}$$

and this choice ensures that the initial guess is not too close to the exact values $T^{(\mathrm{an})}$.

6.3 Convergence of the algorithm

In order to investigate the convergence of the proposed CGM + BEM algorithm, at every iteration we evaluate the accuracy errors defined by

$$\begin{aligned} e_T &= \| T^{(k)} - T^{(\mathrm{an})} \|_{H^{1/2}(\Gamma_1)}, \\ E_T &= \| A T^{(k)} - T^{(\mathrm{an})} \|_{L^2(\Gamma_2)} \ , \end{aligned} \tag{42}$$

where $T^{(k)}$ is the temperature on the boundary Γ_1 retrieved after k iterations, the linear operator A is given by Eq. (4) and each iteration consists of solving three direct, mixed, well-posed problems as described in Sect. 4.

Figure 1(a) and (b) show the accuracy errors e_T and E_T, respectively, as functions of the number of iterations, k, obtained for the Cauchy problem given by example 1 for $N \in \{40, 80, 160\}$ boundary elements when using "exact boundary data" for the inverse problem, i.e. boundary data obtained by solving a direct well-posed problem, namely

$$\begin{cases} LT(\underline{x}) = 0, & \underline{x} \in \Omega \\ \frac{\partial T}{\partial n}(\underline{x}) = \frac{\partial T^{(\mathrm{an})}}{\partial n}(\underline{x}), & \underline{x} \in \Gamma_1 \\ T(\underline{x}) = T^{(\mathrm{an})}(\underline{x}), & \underline{x} \in \Gamma_2 \ . \end{cases} \tag{43}$$

From these figures it can be seen that both errors e_T and E_T keep decreasing, even after a large number of iterations, e.g. $k = 1000$. Furthermore, for example 1, $N \geq 40$ ensures a sufficient discretisation for the accuracy to be achieved. It should also be noted that the pattern of the convergence

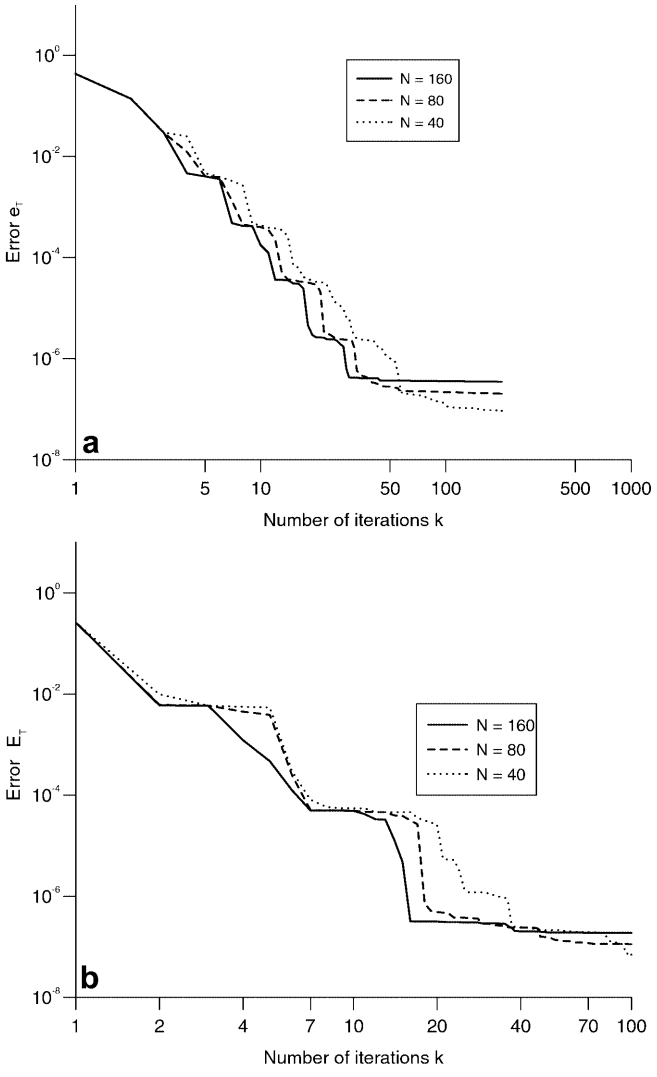

Fig. 1. The errors **(a)** $e_T = \|T^{(k)} - T^{(\mathrm{an})}\|_{H^{1/2}(\Gamma_1)}$, and **(b)** $E_T = \|AT^{(k)} - T^{(\mathrm{an})}\|_{L^2(\Gamma_2)}$ as functions of the number of iterations, k, obtained with $N = 40(\cdots)$, $N = 80$ (– –), and $N = 160$ (—) constant boundary elements, for the Cauchy problem considered in example 1

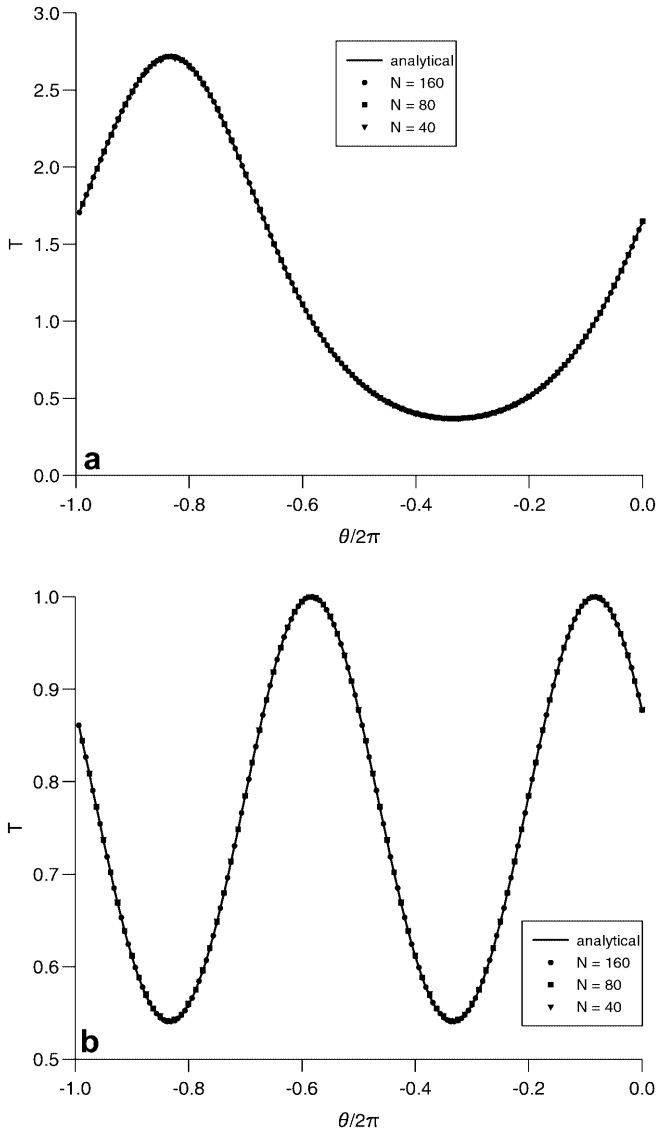

Fig. 2. The analytical solution $T^{(\mathrm{an})}$ (—) and the numerical solution obtained with $N = 40$ (▼), $N = 80$ (■), and $N = 160$(●) constant boundary elements, on the underspecified boundary Γ_1, for the Cauchy problem considered in **(a)** example 1, and **(b)** example 2

process, with sharp decreases followed by flat portions is common to conjugate gradient methods, see e.g. Hào and Lesnic [23] and Marin et al. [24]. Similar results have been obtained for the Cauchy problem given by example 2 and therefore they are not presented herein.

The numerical solutions for the temperature $T|_{\Gamma_1}$ obtained after $k = 1000$ iterations for the Cauchy problems given by examples 1 and 2 are presented in Figure 2(a) and (b), respectively. From these figures, it can be seen that the accuracy in predicting the temperature distribution on the boundary Γ_1 is very good for both examples considered. Although not illustrated here, an important conclusion is reported, namely that the numerical solution for the temperature $T|_{\Gamma_1}$ is more accurate for the Cauchy problem in an annulus, i.e. examples 1 and 2, than for the Cauchy problem in a disk, see e.g. Hào and Lesnic [23] and Marin et al. [24]. The reason for this is that $\overline{\Gamma}_1 \cap \overline{\Gamma}_2 = \emptyset$ in the case of examples 1 and 2, whilst $\overline{\Gamma}_1 \cap \overline{\Gamma}_2 \neq \emptyset$ in the case of a disk, i.e. there exist two points where the constant BEM changes to mixed boundary conditions. It is well known, see e.g. Fichera [29] and Schiavone [30], that the gradient of the temperature T possesses singularities at the points where the data changes from temperature boundary conditions to flux boundary conditions, even if the temperature and the flux data are of class $\mathscr{C}^\infty$. Consequently, the classical solution for the temperature T cannot be smooth, although its smoothness can be improved if the temperature and the flux data are required to satisfy an increasing number (increasing with smoothness) of additional conditions, see also Wendland et al. [31]. Nevertheless, in the numerical implementation one may use linear boundary elements to enforce a smooth temperature across the junctions $\overline{\Gamma}_1 \cap \overline{\Gamma}_2$ or, even better, weighted functions at each iteration of the

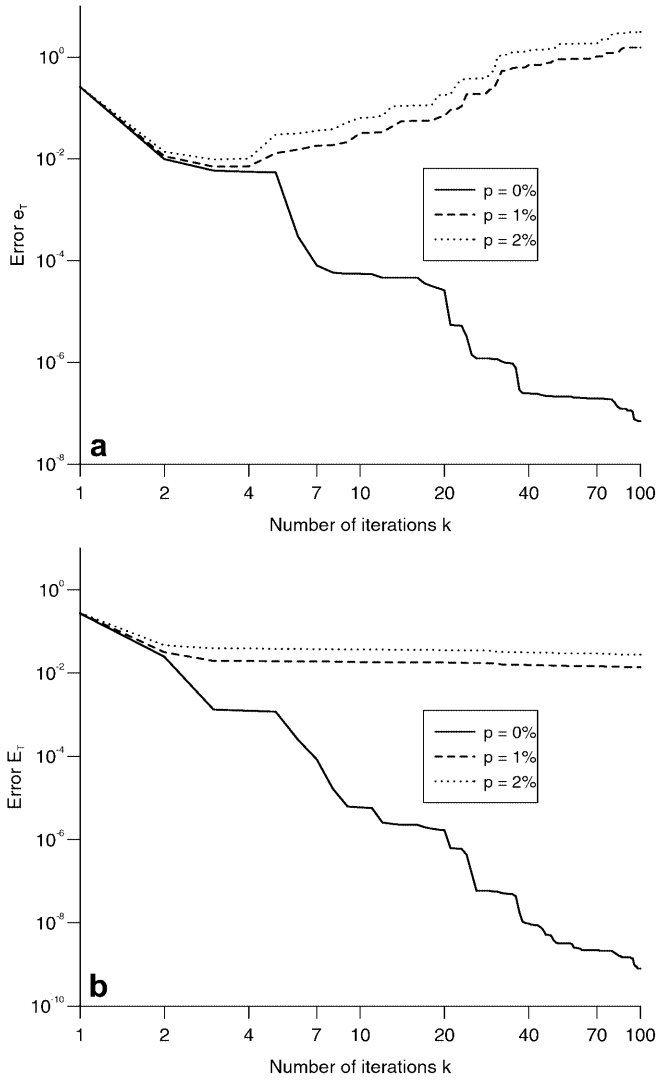

Fig. 3. The errors **a** $e_T = \|T^{(k)} - T^{(\mathrm{an})}\|_{H^{1/2}(\Gamma_1)}$, and **b** $E_T = \|AT^{(k)} - T^{(\mathrm{an})}\|_{L^2(\Gamma_2)}$ as functions of the number of iterations, k, obtained with $N = 40$ constant boundary elements and several amounts of noise, namely $p = 0\%$ (—), $p = 1\%$ (– –) and $p = 2\%$ $(\cdots)$ added into the input data $\tilde{T}|_{\Gamma_2}$, for the Cauchy problem considered in example 2

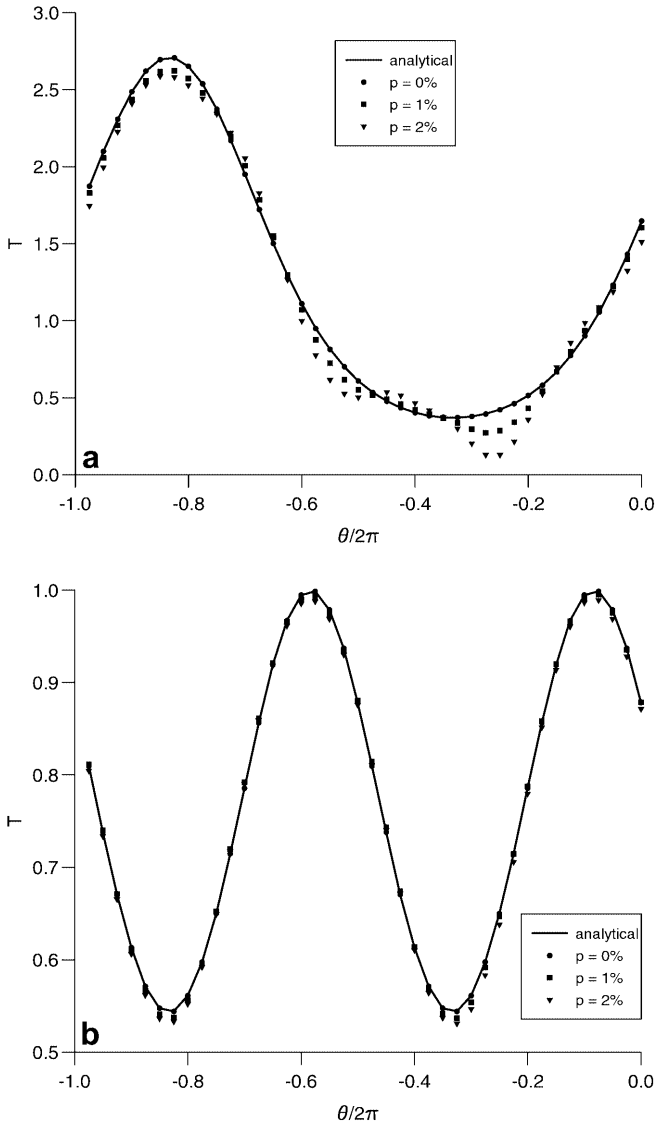

Fig. 4. The analytical solution $T^{(\mathrm{an})}$ (—) and the numerical solution obtained with $N = 40$ constant boundary elements and several amounts of noise $p = 0\%$ (●), $p = 1\%$ (■), and $p = 2\%$ (▼) added into the input data $\tilde{T}|_{\Gamma_2}$, for the Cauchy problem considered in **a** example 1, and **b** example 2

algorithm in order to cancel the singularity, but this will be investigated in a future work.

For the Cauchy problem investigated in this paper, it was found that the proposed CGM + BEM algorithm produces an accurate and convergent numerical solution for the missing boundary temperature with respect to increasing the number of iterations, k, and the number of boundary elements, N, provided that exact input data is used. However, exact data is seldom available in practice since measurement errors always include noise in the prescribed boundary conditions and this is investigated next.

6.4 Stability of the algorithm

Once the convergence with respect to increasing k of the numerical solution to the exact solution has been established, we fix $N = 40$ and investigate the stability of the numerical method proposed by perturbing the input boundary temperature data $T|_{\Gamma_2}$ as $\overline{T}|_{\Gamma_2} = T|_{\Gamma_2} + \delta T$, where δT is a Gaussian random variable with mean zero and standard deviation $\sigma = (p/100) \max_{\Gamma_2} |T|$, generated by the NAG subroutine G05DDF, and p is the percentage of additive noise included in the input data $T|_{\Gamma_2}$ in order to simulate the inherent measurement errors.

Figure 3(a) and (b) illustrate the accuracy errors e_T and E_T, respectively, for various levels of Gaussian noise $p \in \{0, 1, 2\}\%$ added into the temperature data $T|_{\Gamma_2}$ corresponding to the Cauchy problem given by example 2. From these figures it can be seen that as p decreases then both e_T and E_T decrease. However, the error e_T in predicting the temperature on the underspecified boundary Γ_1 and the error E_T in the residual temperature on the overspecified boundary Γ_2 decrease up to a certain iteration number after which they start increasing. If the

Table 1. Optimal iteration numbers and errors for $N = 40$ boundary elements and various amounts $p \in \{0, 1, 2\}$ of noise added into the input data $\widetilde{T}|_{\Gamma_2}$, for the Cauchy problems considered in examples 1 and 2

Problem	p	0%	1%	2%
Example 1	ε	0.00	1.99×10^{-1}	3.98×10^{-1}
	k_N	∞	3	3
	$e_T(k_N)$	1.00×10^{-6}	1.04×10^{-1}	2.16×10^{-1}
	$E_T(k_N)$	2.25×10^{-8}	1.42×10^{-1}	2.83×10^{-1}
Example 2	ε	0.00	3.01×10^{-2}	6.02×10^{-2}
	k_N	∞	3	2
	$e_T(k_N)$	1.14×10^{-6}	7.01×10^{-3}	1.38×10^{-2}
	$E_T(k_N)$	5.61×10^{-8}	1.96×10^{-2}	4.66×10^{-2}

iterative process is continued beyond this point then the numerical solution loses its smoothness and becomes highly oscillatory and unbounded, i.e. unstable. Therefore, a regularising stopping criterion, such as Nemirovskii's stopping criterion (27), must be used in order to terminate the iterative process at the point where the error in the numerical solution starts increasing.

In Figures 4(a) and (b) we present the numerical results obtained for the temperature T on the boundary Γ_1 for various levels of noise added into the temperature data on the boundary Γ_2, namely $p \in \{0, 1, 2\}$, corresponding to the Cauchy problems given by examples 1 and 2, respectively. From these figures, it can be seen that the numerical solution is a stable approximation to the exact solution, free of unbounded and high oscillations. The same conclusion can be drawn from Table 1 which presents the errors e_T and E_T obtained for the Cauchy problems given by examples 1 and 2 for various levels of noise added into the temperature data on Γ_2, as well as the values of ε and the optimal iteration numbers, k_N, according to the stopping criterion (27), as suggested by Nemirovskii.

From the numerical results presented in this section, it can be concluded that Nemirovskii's stopping criterion (27) has a regularising effect and the numerical results obtained by the CGM + BEM algorithm described in Section 4 are convergent and stable with respect to refining the the mesh size discretisation and decreasing the amount of noise added into the input data, respectively.

7 Conclusions

In this paper, we have formulated the Cauchy problem for Helmholtz-type equations in a variational form where only weak requirements for the Cauchy data are required. Consequently, the solution of the direct problems, as well as the associated adjoint problems, are defined in a weak sense and a mathematical analysis has been undertaken. The variational approach for solving the Cauchy problem of Helmholtz-type equations needs the gradient of the minimisation functional, which is provided by the solution of the adjoint problem.

Due to the explicit representation of the gradient, the CGM was employed to solve numerically the Cauchy problem. The algorithm proposed consists of solving three direct, mixed, well-posed problems for Helmholtz-type equations at every iteration but because of the linearity of the problem only two direct solutions are required at every iteration. In combination with Nemirovskii's stopping criterion, the CGM is known to be of optimal order when the data is sufficiently smooth. The numerical implementation of the CGM is accomplished by using the BEM, which requires the discretisation of the boundary only. Cauchy problems are inverse boundary value problems and thus the BEM is a very suitable method for solving such improperly posed problems. From the discussion of the results obtained for two benchmark examples, it can be concluded that the CGM with an appropriate stopping rule together with the BEM produce a convergent, stable and consistent numerical solution with respect to increasing the number of boundary elements and decreasing the amount of noise added into the input Cauchy data.

References

1. **Beskos DE** (1997) Boundary element method in dynamic analysis: Part II (1986–1996). ASME Appl. Mech. Rev. 50: 149–197
2. **Chen JT, Wong FC** (1998) Dual formulation of multiple reciprocity method for the acoustic mode of a cavity with a thin partition. J. Sound Vibration 217: 75–95
3. **Harari I, Barbone PE, Slavutin M, Shalom R** (1998) Boundary infinite elements for the Helmholtz equation in exterior domains. Int. J. Numer. Meth. Eng. 41: 1105–1131
4. **Hall WS, Mao XQ** (1995) A boundary element investigation of irregular frequencies in electromagnetic scattering. Eng. Anal. Bound. Elem. 16: 245–252
5. **Kern DQ, Kraus AD** (1972) Extended Surface Heat Transfer. McGraw-Hill, New York
6. **Manzoor M, Ingham DB, Heggs PJ** (1983) The one-dimensional analysis of fin assembly heat transfer. ASME J. Heat Transfer 105: 646–651
7. **Lin CN, Jang JY** (2002) A two-dimensional fin efficiency analysis of combined heat and mass transfer in elliptic fins. Int. J. Heat Mass Transfer 45: 3839–3847
8. **Niwa Y, Kobayashi S, Kitahara M** (1982) Determination of eigenvalue by boundary element method. In: Banerjee PK, Shaw R (eds) Development in Boundary Element Methods. Chapter 7. Applied Science Publisher, New York
9. **De Mey G** (1977) A simplified integral equation method for the calculation of the eigenvalues of Helmholtz equation. Int. J. Numer. Meth. Eng. 11: 1340–1342
10. **Hutchinson JR** (1985) An alternative BEM formulation applied to membrane vibrations. In: Brebbia CA, Maier G (eds) Boundary Elements VII. Springer Verlag, Berlin, pp. 613–625
11. **Nowak AJ, Brebbia CA** (1989) Solving Helmholtz equation by boundary elements using multiple reciprocity method. In: Calomagno GM, Brebbia CA (eds) Computer Experiment in Fluid Flow. CMP/Springer Verlag, Berlin, pp. 265–270
12. **Kamiya N, Andoh E** (1993) Eigenvalue analysis by boundary element method. J. Sound Vibration 160: 279–287
13. **Kamiya N, Andoh E, Nogae K** (1993) Eigenvalue analysis by boundary element method: New developments. Eng. Anal. Bound. Elem. 16: 203–207
14. **Nardini CF, Brebbia CA** (1983) A new approach to free vibration analysis using boundary elements. In: Brebbia CA, Futagami T, Tanaka M (eds) Boundary Elements V. Springer Verlag, Berlin, pp. 719–730
15. **Agnantiaris JP, Polyzer D, Beskos D** (1998) Three-dimensional structural vibration analysis by the dual reciprocity BEM. Comput. Mech. 21: 372–381

16. **Golberg MA, Chen CS, Bowman H, Power H** (1998) Some comments on the use of radial basis functions in the dual reciprocity method. Comput. Mech. 22: 61–69
17. **Chen G, Zhou J** (1992) Boundary Element Methods. Academic Press, London
18. **Bai MR** (1992) Application of BEM-based acoustic holography to radiation analysis of sound sources with arbitrarily shaped geometries. J. Acoust. Soc. Am. 92: 533–549
19. **Kim BK, Ih JG** (1996) On the reconstruction of the vibroacoustic field over the surface enclosing an interior space using the boundary element method. J. Acoust. Soc. Am. 100: 3003–3016
20. **Wang Z, Wu SR** (1997) Helmholtz equation-least-squares method for reconstructing the acoustic pressure field. J. Acoust. Soc. Am. 102: 2020–2032
21. **Wu SR, Yu J** (1998) Application of BEM-based acoustic holography to radiation analysis of sound sources with arbitrarily shaped geometries. J. Acoust. Soc. Am. 104: 2054–2060
22. **DeLillo T, Isakov V, Valdivia N, Wang L** (2001) The detection of the source of acoustical noise in two dimensions. SIAM J. Appl. Math. 61: 2104–2121
23. **Hào DN, Lesnic D** (2001) The Cauchy problem for Laplace's equation via the conjugate gradient method. IMA J. Appl. Math. 65: 199–217
24. **Marin L, Hào DN, Lesnic D** (2002) Conjugate gradient-boundary element method for the Cauchy problem in elasticity. Q. Jl. Mech. Appl. Math. 55: 227–247
25. **Nemirovskii AS** (1986) The regularizing properties of the adjoint gradient method in ill-posed problems. Comput. Maths. Math. Phys. 26: 7–16
26. **Hadamard J** (1923) Lectures on Cauchy Problem in Linear Partial Differential Equations. Oxford University Press, London
27. **Lions JL, Magenes E** (1972) Non-Homogeneous Boundary Value Problems and Their Applications. Springer Verlag, Berlin
28. **Hanke M, Hansen PC** (1993) Regularization methods for large-scale problems. Surveys Math. Industry 3: 253–315
29. **Fichera G** (1952) Sul problema della derivata obliqua e sul problema misto per l'equazione di Laplace. Boll. Un. Mat. Ital. 7: 367–377
30. **Schiavone P** (1997) Mixed problem in the theory of elastic plates with transverse shear deformation. Q. J. Mech. Appl. Math. 50: 239–249
31. **Wendland WL, Stephan E, Hsiao GC** (1979) On the integral equation method for the plane mixed boundary value problem for the Laplacian. Math. Meth. Appl. Sci. 1: 265–321